Supporting Information

Zhang et al. 10.1073/pnas.0913403107

SI Text

Arrangement of the Coat VP2 and VP5 Proteins and the Core VP7 and VP3 Proteins. Consistent with prior findings (1), each triangular face of the icosahedral structure (Fig. 1*C*), with three asymmetrical units, contains three of the outer coat VP2 triskelia (=9 monomers) (magenta in the top panel of Fig. 1*C*), 6 trimers (=18 monomers) of inner coat VP5 (green and cyan in the top panel), 13 trimers (=39 monomers) of the outer core VP7 (green P, cyan Q, blue R, yellow S, and red T in the middle panel), and 6 monomers of the inner core VP3 (cyan and green in the bottom panel), a total of 72 proteins, giving nominal triangulation (T) numbers of 3, 6, 13, and 2.

Each (magenta) VP2 triskelion has one "hub" and three "tip" domains. Each hub sits above the VP7 trimer in position Q (cyan in the middle panel of Fig. 1*C*), and the three VP2 tip domains sit above VP7 trimers in positions P (green), R (blue), and S (yellow). No VP2 protein sits above the VP7 trimer in position T (red), permitting one to see the (red) trimer in the middle of Fig. 1*B* through the VP2 layer.

The two (cyan/A and green/B) quasi-equivalent inner-coat VP5 trimers sit above the channels labeled III and II, respectively, in the outer core VP7 array (middle panel of Fig. 1*C*) (1).

Similarly, the outer core VP7 array is stacked above the two (cyan and green) monomers of the inner core VP3 array (bottom panel of Fig. 1*C*) in a specific manner, with the three cyan VP3 monomers toward the periphery of each triangular face and the three green VP3 monomers toward the center of each triangular face.

Interaction Between a VP2 Attachment Triskelion in the Outer Coat and Three VP5 Penetration Trimers in the Inner Coat. Each VP2 monomer's hub domain interacts extensively with the other two monomers' hub domains (Fig. 2*A*) to form the hub that holds the VP2 triskelion together. The resulting VP2 triskelion has three legs and therefore three gaps between them. Two are occupied by (cyan) VP5.A conformers and one by a (green) VP5.B conformer (Fig. 1*C Top* and Fig. S7*A*). As noted above, there are two quasi-equivalent types of VP5 trimer, which are colored cyan and green in the top panel of Fig 1*C*.

Interactions can be seen in the density map exclusively between VP2 hub domains and VP5 trimers—VP2 tip domains do not participate. The interaction consists of thin fingers of density. Just one finger connects the VP2 triskelion to one of the (cyan) VP5.A conformers (VP5.A1), just three fingers connect the VP2 triskelion to the other (cyan) VP5.A conformer (VP5.A2), and just three fingers connect the VP2 triskelion to the VP5.B conformer (Fig. S6 and Table S1). The interaction between outer-coat VP2 and inner-coat VP5 thus appears to be weak.

Interaction Between a VP5 Penetration Trimer in the Inner Coat and Five VP7 Trimers in the Outer Core. The establishment of the fold of the VP5 penetration trimer in the inner coat permits us to identify structures that interact with the subjacent VP7 trimers in the outer core. These interaction sites are of particular interest because their identification enables designing of stable vaccines with enhanced interactions that reduce uncoating.

The A (cyan) and B (green) VP5 conformers are located above the channels labeled III and II, respectively (1, 2), marked by cyan and green triangles in the VP7 layer of the outer core (middle panel of Fig. 1*C* and Fig. S7*A*). Each type III channel (cyan triangle) is surrounded by six VP7 trimers (Fig. S7*A*), three at corners and three along edges of the VP7 triangle; however, we see no interaction along one edge (with VP7.Q3). Each type II channel (green triangle) is also surrounded by six VP7 trimers (Fig. S7*A*), three at corners of the VP7 triangle and three along edges; however, the interaction along one edge (with VP7.S2) is missing (2).

Thin fingers of density extend within the cryoEM density map from cyan and green inner coat VP5 penetration trimers to five of the six VP7 trimers in the ring below (Fig. S7 *B* and *C*). These interactions, summarized in Tables S2 and S3, include nine between the cyan (A) inner coat VP5 trimer and its five subjacent outer core VP7 neighbors and another ten between the green (B) inner coat VP5 and its five subjacent outer core VP7 neighbors. In keeping with symmetry, we find consistent interaction partners at some sites between monomers of VP5 trimers and monomers of the corner VP7 trimers [e.g., in Tables S2 and S3: yellow highlighted boxes in VP5 (from the middle of #30L, around Lys344) to cyan highlighted boxes in VP7 (one β-strand of a β-sheet, around Gly166 to Arg168)]. In keeping with quasi-equivalence, however, we find many interactions that are one of kind between sites on VP5 monomers and sites on VP7 monomers. Among the latter, we find one-to-many interactions [particular sites on VP5 (e.g., orange highlighted boxes) that interact with both cyan and green highlighted sites on VP7] and many-to-one interactions [a variety of sites on VP5 that interact with the same site (e.g., blue highlighted sites) on VP7].

Interaction Between a VP2 Triskelion in the Outer Coat and Four VP7 Trimers in the Outer Core. The VP2 triskelion hub in the outer coat sits above the top of a VP7 trimer in the Q position (cyan in Fig. 2*B* and Fig. S7*A*, labeled in Fig. S8*A*), and each of the VP2 triskelion's three tip domains sits above a VP7 trimer in the P, R, or S position (green P, blue R, or yellow S in Fig. 2*B* and Fig. S7*A*; labeled in S8*A*). Moderately thick fingers of density connect each tip domain to its underlying VP7 trimer, whereas a wall of density connects the hub to its underlying VP7.Q trimer (Fig. S8*A*). Because the outer core VP7 is available at atomic resolution, we and Nason et al. (1) were able to identify a moderate number of contact residues provided by VP7 trimers for interaction with the VP2 tip domains and a large number of contact residues provided by the VP7.Q trimer for interaction with the VP2 hub (Fig. S8*B*). Nonetheless, the coat detaches readily from the core at high salt concentration (1).

Lectin Staining and Competition. Hela cells were chilled to 4 °C and then incubated with 10 μg/mL of WGA in DMEM. Cultures were incubated at 4 °C for 20 min, rinsed three times with DMEM, rinsed three times with PBS, and fixed with 4% paraformaldehyde in PBS. Nuclei were stained with Hoechst 33258 (Sigma), and the expression of nonstructural protein 2 (NS2) (red) was detected by incubation with a guinea pig polyclonal antiserum raised to NS2, followed by incubation with a TRITC-conjugated anti-guinea pig IgG (Sigma). In infectivity competition experiments, HeLa cells were preincubated at 4 °C with 100 μg/mL of WGA in DMEM for 10 min. The preincubation solution was removed, and DMEM containing 100 μg/mL of WGA and BTV-1 (MOI 1 pfu/mL) was added. Cultures were incubated at 4 °C for 1 h first, rinsed, and incubated at 37 °C for 16 h.

WGA-treated and BTV-1 infected Hela cells were washed with cold PBS, fixed, permeabilized, and immunolabeled as described previously (3). After being labeled, the samples were mounted

using Gel Mount Aqueous Mounting Medium (Sigma) and analyzed with a Zeiss LSM 510 confocal microscope. The images were obtained with LSM 510 image browser software and processed using Photoshop Elements 2.0 (Adobe).

To examine the effect of WGA on virus yield, viruses from both BTV-infected and WGA-treated cells were collected at 16 h post-infection, and virus titers were determined by plaque assay on baby hamster kidney cells. The viral titer was normalized to the titer obtained for untreated infected cells. The mean and standard error of the reduction mediated by WGA were calculated using Sigma Plot 2000 (Systat Software Inc.).

Secondary Structural Elements Prediction for VP5 and Mapping to the cryoEM Structure. Jpred (4) and PSIPRED (5) were used to predict secondary structural regions from the 526 amino acid sequence of VP5. Helical Wheel (http://www.site.uottawa.ca/~turcotte/resources/HelixWheel/) was used to identify amphipathic regions of predicted α-helixes (Fig. S4), and modeling and visualization of protein structures were performed with UCSF Chimera (6).

To map these secondary structure predictions to the secondary structures revealed in the cryoEM density map, we began by noting that several of the α-helixes or sets of contiguous α-helices in the amino acid sequence are very long, ≥40 amino acids (amino acids 4–19/23–60, 91–135, 169–232, and 296–335) (Fig. 4*B*). Correspondingly, several of the helix densities or contiguous groups of helix densities in the cryoEM structure are very long, ≥10 helical turns (#1H-3H, #7H-12H, #17H, and #27H-29H). The first of these α-helix groups, at the N-terminal end of the amino acid sequence, was assigned to helices #1H-3H in the 3D model, a long helix density that also comes to an end at the N terminus (Fig. 5*A*, blue sphere). The third of these α-helices is the longest and was tentatively assigned to the longest helix density in the 3D model, helix #17H. We then followed in tandem the secondary structural elements (α-helices, loops, and β-strands) in the amino acid sequence and in the cryoEM density map, including our prior assignment of helices, loops, and the β-sheet. By this method we built a model of the 3D fold of the secondary structural elements of VP5—with the exception of the two carboxy terminal-most (hydrophobic) α-helices in the amino acid sequence (Fig. 4*B*), which we presume to be disordered. For this reason, the location of the black sphere at the end of 41H in Fig. 5*A* represents the last resolved structure at the C-terminal end. In addition, due to the difficulty in resolving loops near the region of the β-sheet, our confidence in loops labeled 30L is not high.

1. Nason EL, et al. (2004) Interactions between the inner and outer capsids of bluetongue virus. *J Virol* 78:8059–8067.
2. Grimes JM, et al. (1998) The atomic structure of the bluetongue virus core. *Nature* 395:470–478.
3. Bhattacharya B, Roy P (2008) Bluetongue virus outer capsid protein VP5 interacts with membrane lipid rafts via a SNARE domain. *J Virol* 82:10600–10612.
4. Cole C, Barber JD, Barton GJ (2008) The Jpred 3 secondary structure prediction server. *Nucleic Acids Res* 36:W197–201.
5. Bryson K, et al. (2005) Protein structure prediction servers at University College London. *Nucleic Acids Res* 33:W36–38.
6. Pettersen EF, et al. (2004) UCSF Chimera—a visualization system for exploratory research and analysis. *J Comput Chem* 25:1605–1612.
7. Rosenthal PB, Henderson R (2003) Optimal determination of particle orientation, absolute hand, and contrast loss in single-particle electron cryomicroscopy. *J Mol Biol* 333:721–745.

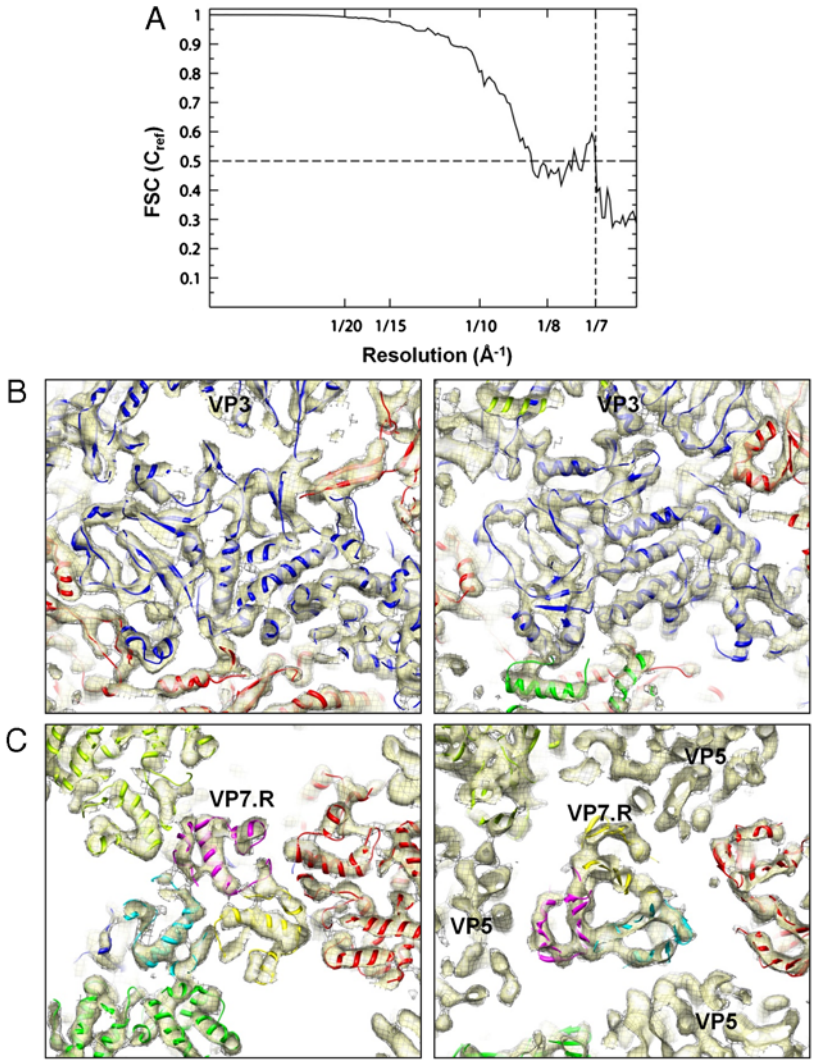

Fig. S1. Resolution assessments. (*A*) The modified Fourier shell correlation coefficient, C_{ref}, as defined by Rosenthal and Henderson (7). According to the $C_{ref} = 0.5$ criterion, the effective resolution of the reconstruction of the whole virion is estimated at 7 Å. (*B*, *C*) Agreement between the secondary structural elements revealed in our cryoEM density maps (mesh, contoured at 1.3σ) and those identified in the atomic resolution structure (ribbon) (2). Shown here are 15-Å-thick slabs of the superimposed structures containing inner core VP3 regions (*B*) at radii 245 (*Left*, B) and 265 Å (*Right*, B), and those containing regions of a VP7.R trimer in the outer core at radii 290 (*Left*, C) and 340 Å (*Right*, C).

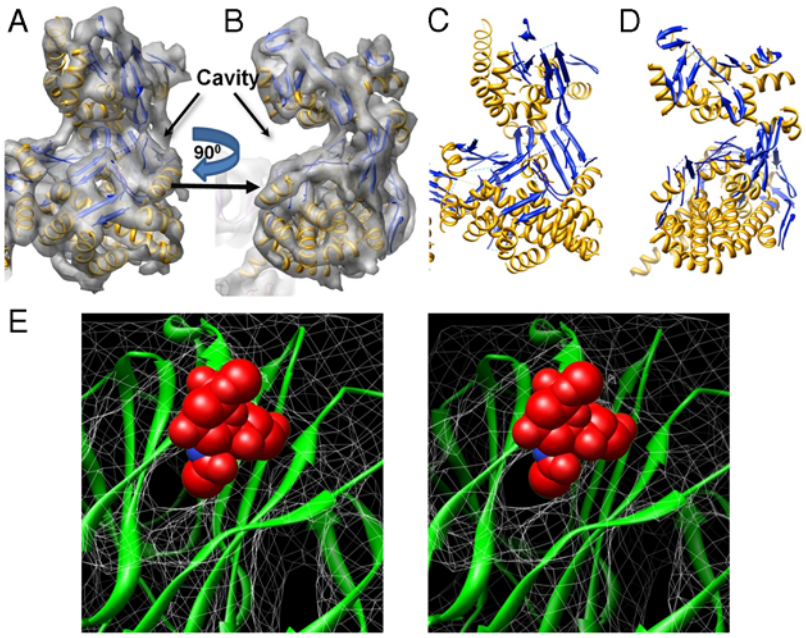

Fig. S2. The tip and the sialic acid (SA) binding domains of VP2. (*A*) Side view of the tip domain of a VP2 monomer, rotated slightly about the vertical axis from Fig. 2*B*. (*B*) Another side view, rotated 90° about the vertical axis from (*A*). Secondary structural elements are shown as ribbons (orange helices and blue β-strands) embedded in the density maps (*A*, *B*) and shown by themselves (*C*, *D*). A cavity lined by β-sheets is evident in the top half of the tip domain. (*E*) SA binds to the cleft of the β-barrel in each of the three hub domains of a VP2 triskelion. Stereo Fig. 2*E* shows the docking of the atomic resolution ribbon model of the SA-binding domain of VP8 from rotavirus into the density map (contour level = 1.5σ) of the hub domain of a VP2 monomer in BTV. This stereo figure adds a molecule of SA in the position determined from crystallography of VP8 of rotavirus, showing that SA would sit in the β-barrel of VP2 of BTV.

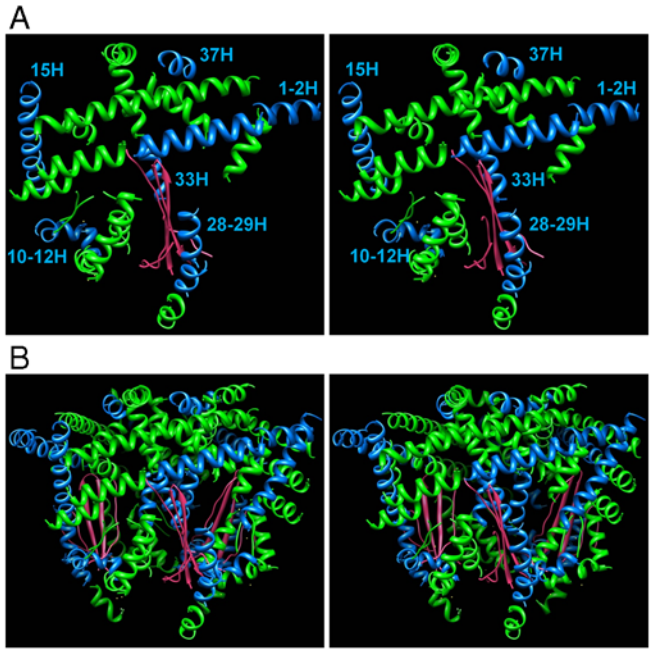

Fig. S3. Stereopairs of the ribbon models of VP5 with only the identified helices and sheets. These side views are based on a mapping of the secondary structures predicted from the amino acid sequence to the secondary structures revealed by the cryoEM density map. In this side view of a ribbon model of a VP5 monomer (*A*) and of a VP5 trimer (*B*), amphipathic helices are shown in blue (and numbered in *A*); all other helices are shown in green; β-strands are shown as thick pink arrows.

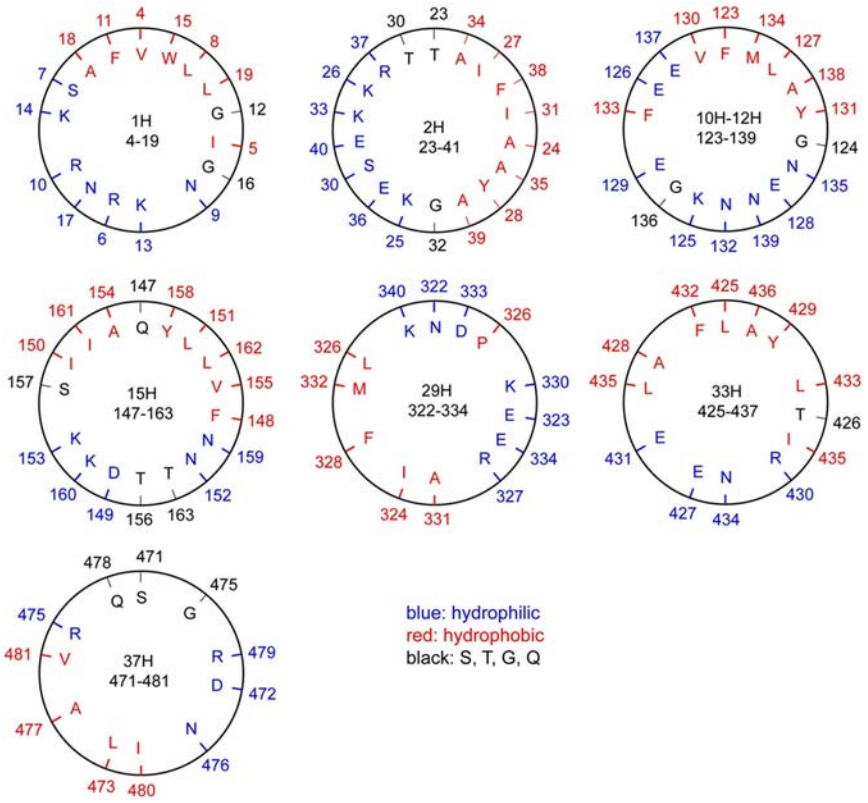

Fig. S4. Amphipathic helix wheels in VP5. Identification of amphipathic sequences within predicted α-helices is based on Helical Wheel software. Blue colored text represents hydrophilic amino acids, red represents hydrophobic, and black represents the amino acids coded S (Ser), T (Thr), G (Gly), and Q (Gln).

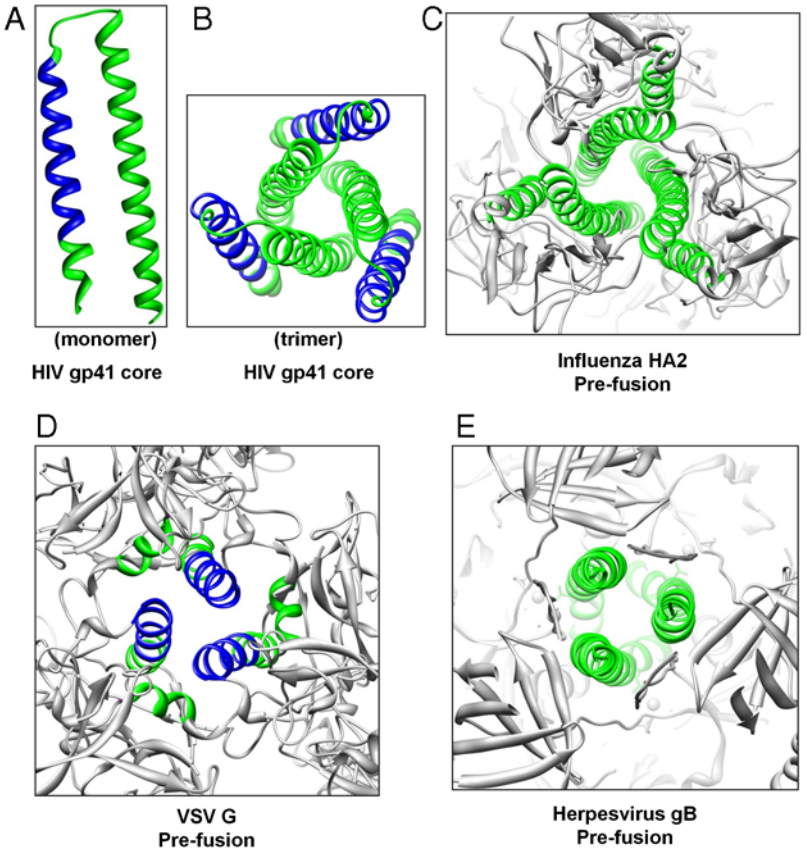

Fig. S5. Ribbon diagrams of the central coiled-coil helix bundle in fusion proteins of enveloped viruses. Blue ribbons represent amphipathic regions of α-helices; green ribbons represent nonamphipathic regions of α-helices. (*A*) The all-green (not amphipathic) helix is one of three central helices; the blue and green helix is one of three peripheral helices. (*B*) The trimer of the monomer shown in (*A*). (*C*, *D*, *E*) Trimers of central and peripheral helices in fusion proteins of other viruses.

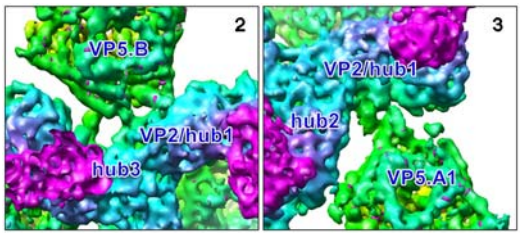

Fig. S6. Interaction between a VP2 triskelion (in the outer coat) and three VP5 penetration trimers (in the inner coat). The two boxes (**2** and **3**) are enlargements of the boxes with the same numbers from Fig. 5. The VP5.B conformer in box 2 connects by three thin fingers of density to two VP2 hub domains numbered 1 and 3. The VP5.A conformer in box 3 connects by one thin finger of density to one VP2 hub domain numbered 1. See Table S1.

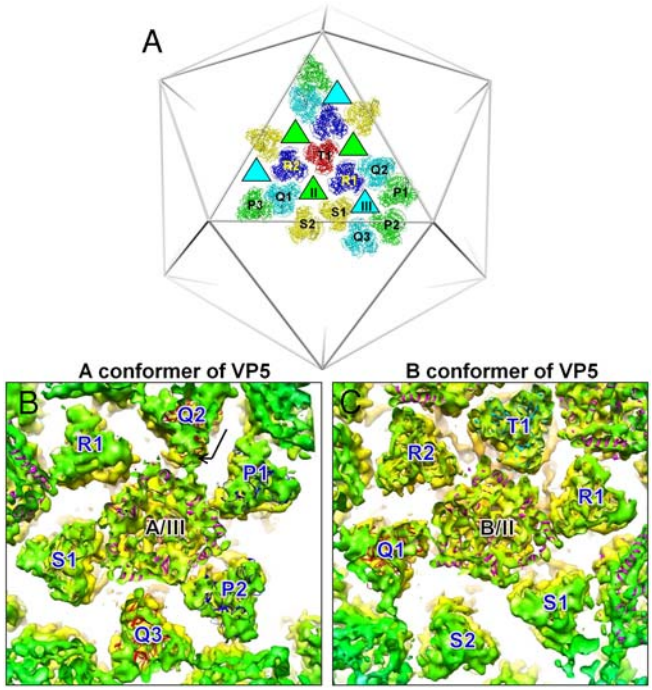

Fig. S7. Interaction between a VP5 penetration trimer (in the inner coat) and five VP7 trimers (in the outer core). (*A*) The A and B conformers of VP5, respectively, sit atop channels III (cyan triangle) and II (green triangle). Each VP5 penetration trimer is surrounded by six VP7 trimers (labeled to indicate the equivalence (e.g., Q2 and Q3) and quasi-equivalence (e.g., Q2 and P1). (*B*) A small number of thin fingers of density (e.g., arrow) connect each VP7.A trimer to five of its six subjacent VP5 trimers, missing VP5.Q3. (*C*) A small number of thin fingers of density connect each VP7.B trimer to five of its six subjacent VP5 trimers, missing VP5.S2. See also Table S2 and Table S3.

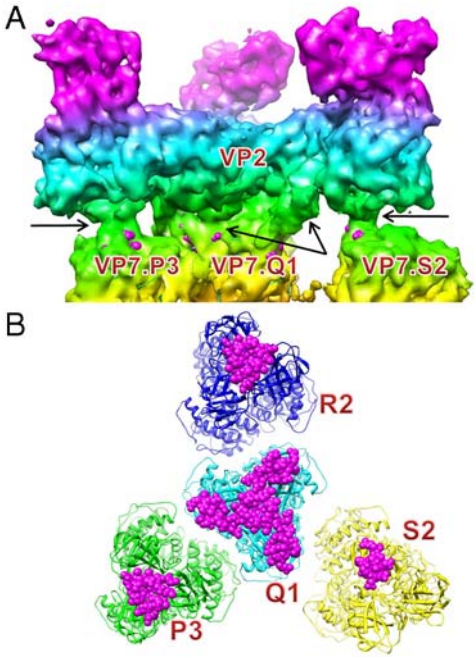

Fig. S8. Interaction between a VP2 triskelion (in the outer coat) and four VP7 trimers (in the outer core). (*A*) Side view of a VP2 triskelion, the tip domains sitting above the outer halves of VP7 trimers in the P and S positions—the back tip domain sits above a VP7 trimer in the R position and is hidden—and with the hub sitting above the VP7 trimer in the Q position. A moderately thick finger of density connects each tip domain with the top of its VP7 trimer (outer two arrows), but a wall of density connects the hub with the top of its VP7 trimer (central pair of arrows). (*B*) Amino acid residues (spheres) in different VP7 trimers that contact VP2: about 13, 24, 24, and 69 residues in the VP7.S2, VP7.R2, VP7.P3, and VP7.Q1 trimers, respectively.

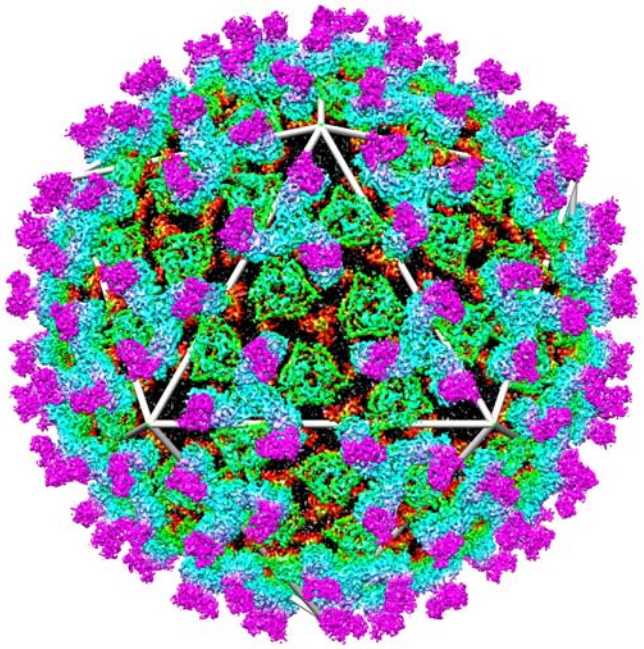

Movie S1. Shaded surface representation of the BTV reconstruction.
Movie S1 (MPG)

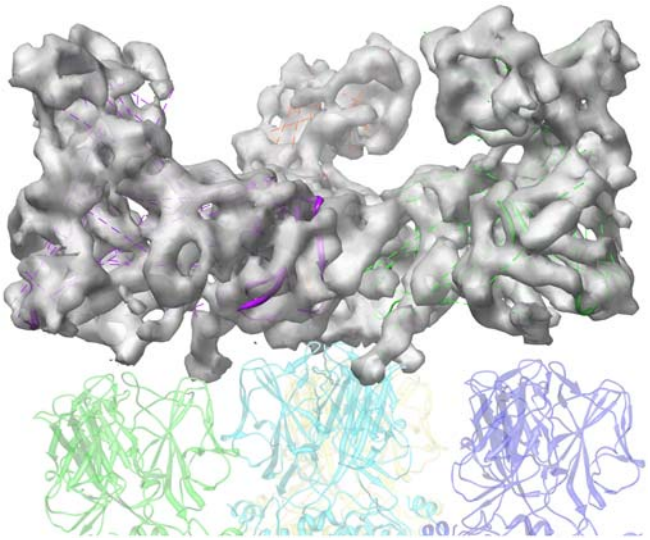

Movie S2. Density map with embedded secondary structures (ribbons) of a VP2 triskelion after 3-fold averaging.
Movie S2 (MPG)

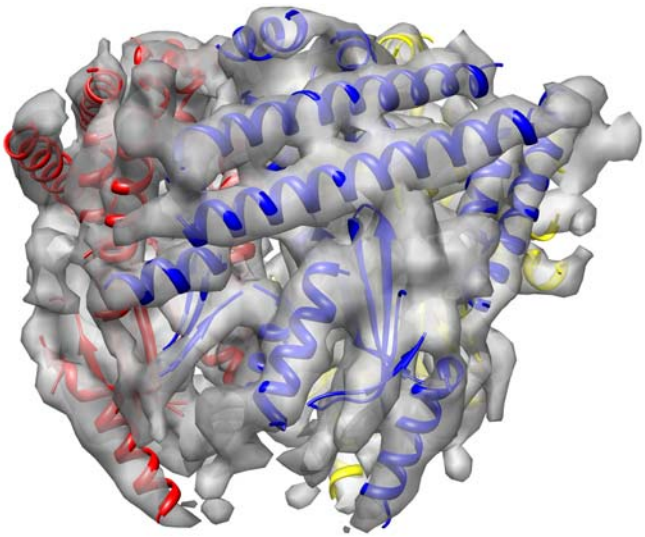

Movie S3. Density map with embedded secondary structures (ribbons) of a VP2 triskelion after 3-fold averaging.
Movie S3 (MPG)

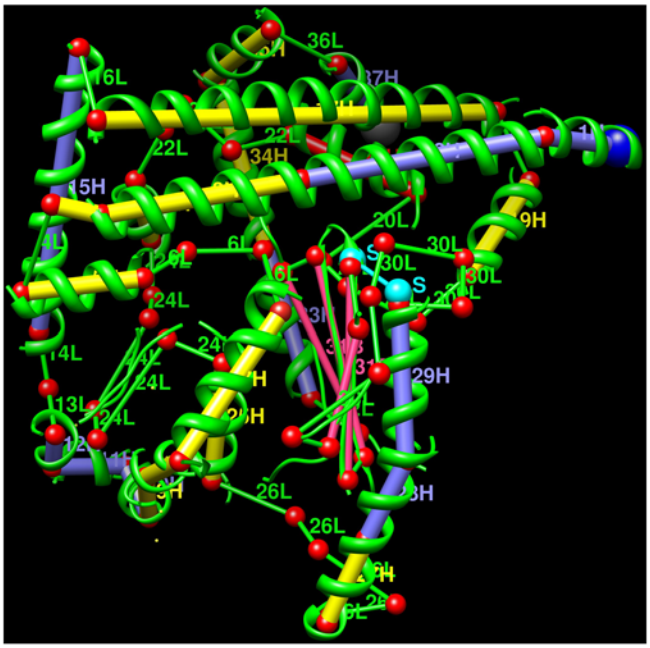

Movie S4. Model of VP5 monomer. In the first part, we show the ribbon model of the secondary structures of a VP5 monomer from the cryoEM density map, along with cylinders that represent the mapping of secondary structures predicted from the amino acid sequence. In the second part, we show only the cylinders. Mapped helices are marked by thick cylinders colored blue (amphipathic), red (hydrophobic), and yellow (others), β-strands in the β-sheet by intermediate thickness cylinders in pink, loops by thin cylinders in green, and the disulfide bond (S-S) by a thin cylinder in cyan.
Movie S4 (MPG)

Table S1. Interaction between the VP2 triskelion (in the outer coat) and the designated conformer in the inner coat

#	VP5 Secondary structure	VP5 Amino acids	Location	VP2 domain
VP5.A1 conformer in the inner coat				
1	Middle of 16L	Asp166	Top of side	Base of Hub1
VP5.A2 conformer in the inner coat				
1	Beginning of 30L	Glu337, near Cys 339	Middle of side	Base of Hub2
2	Beginning of 1H	Lsy3	Top of side	Base of Hub3
3	Middle of 16L	Asp166	Top of side	Base of Hub3
VP5.B conformer in the inner coat				
1	Beginning of 30L	Glu337, near Cys 339	Middle of side	Base of Hub3
2	Beginning of 1H	Lsy3	Top of side	Base of Hub1
3	Middle of 16L	Asp166	Top of side	Base of Hub1

Table S2. Interactions between the inner coat VP5.A (cyan) trimer (above the Type III channel) and subjacent outer core VP7 trimers

Position of VP7 trimer	Location of VP7 with respect to VP5	VP2 domain overlying VP7	VP5 #	VP5 Secondary structure	VP5 Amino acids	VP5 Location	VP7 Secondary structure	VP7 Amino acids
Q2	Corner	hub	1	middle of 30L	Lys344, near Cys339	top of side	one β strand of β sheet	Gly166-Arg168
R1	Side	Tip	2	end of 7H	112Arg	middle of side	β barrel loop	Gln 228
S1	Corner	Tip	3	middle of 30L	Lys344, near Cys339	top of side	one β strand of β sheet	Gly166-Arg168
			4	end of 7H	112Arg	middle of side	Helix	Arg345-Val349
Q3	Side	Hub		None			None	
P2	Corner	Tip	5	middle of 30L	Lys344, near Cys339	top of side	one β strand of β sheet	Gly166-Arg168
							β barrel loop	Arg234
			6	End of 27H	Lys315	side at base	Helix	Arg345-Val349
P1	Side	Tip	7	middle of 3H	Gln53	top of side	one β strand of β sheet	Gly166-Arg168
			8	middle of 1st β strand	His365	middle of side	β barrel loop	Gln 228

Table S3. Interactions between the inner coat VP5.B (green) trimer (above the Type II channel) and subjacent outer core VP7 trimers

Position of VP7 trimer	Location of VP7 with respect to VP5	VP2 domain overlying VP7	VP5 #	VP5 Secondary structure	VP5 Amino acids	VP5 Location	VP7 Secondary structure	VP7 Amino acids
S1	Corner	Tip	1	end 28H	Leu 325	middle of side	β barrel loop	Gly166-Arg168
			2	middle of 30L	Lys344, near Cys339	top of side	β barrel loop	Gln 228
R1	Side	Tip	3	Beginning of 17H	Arg170	top of side	β barrel loop	Asp238
			4	end of 3H	Thr61	top of side	β barrel loop	Arg234
			5	end of 2nd β strand	Arg372-Arg 375	top of side	helix	Arg345-Val349
T1	Corner	None	6	end of 3H	Thr61	top of side	loop	Arg144-Ala148
			7	middle of 30L	Lys344, near Cys339	top of side	β barrel loop	Gly166-Arg168
							β barrel loop	Arg 234
R2	Side	Tip	8	end of 7H	112Arg	middle of side	loop	Val212-Val215
			9	bottom of β sheet	Phe395	side at base	β barrel loop	Gln228-Ala230
Q1	Corner	Hub	10	end of 19H	Glu233	middle of side	one β strand of β sheet	Gly166-Arg168
S2	Side	Tip		None			None	